

MnTiO₃ as a Carbon-Free Cathode for Rechargeable Li–O₂ Batteries

Doaa Aasef Ahmed,^{*a} Mustafa Çelik,^{bc} Wernfried Mayr-Schmölzer,^a Abdulkadir Kızılaslan,^{bc} and Gregor B. Vonbun-Feldbauer^{*ad}

S1 Examining the $U_{\text{H,eff}}$ Value within the GGA+U Functional

In our investigation, we examined U values of 2.5, 3, 3.5, 4, and 4.5 within the GGA+U approach using the PBE functional to accurately determine the band gap, ensuring its consistency with our experimental findings.

The results of our analysis demonstrated that U=3 values yield a band gap (1.56 eV) in excellent agreement with the experimentally observed value (1.58 eV).

S2 Thermal Analysis and Raman Spectroscopy Analyses

The Differential Thermal Analysis (DTA) measurement was carried out with heating rate of 10 °C/min up to 1200 °C under ambient air. The initial weight loss observed below 200 °C and between 200 °C to 350 °C can be attributed to the evaporation of moisture and volatile solvents, followed by the degradation of citric acid respectively. Both thermogravimetric (TG) and differential thermal analysis (DTA) curves exhibit stabilization beyond 400 °C, indicating the complete removal of volatile solvents and organic materials. The DTA curve indicates an equivalent oxidation temperature of 469 °C. Additionally, the DTA curve displays a pronounced endothermic peak at 910 °C, which is associated with the formation of MnTiO₃. Raman spectrum of the synthesized powders was given in Fig S3. The spectrum consists of different peaks denoting the translation, bending and stretching modes within the crystal structure. A_{g1} and E_{g1} represent the stretching of Ti⁴⁺ - O²⁻ bonds. A_{g2} , E_{g2} , A_{g3} , and E_{g3} modes denote the bending motions of O²⁻ - Ti⁴⁺ - O²⁻. A_{g4} and E_{g4} represent the translation of TiO₆ octahedrons against Mn²⁺ cations, whereas A_{g5} and E_{g5} are related to the translation of Mn²⁺ cations against the oxygen framework.¹

S3 Surface stability

To further ascertain the most stable surface, we conduct a comparative analysis between the (104) and (110) surfaces, considering their different terminations.

To determine which termination is likely to emerge from the cleavage of the MnTiO₃ crystal along the (104) and (110) orientation, the cleavage energy (E_{cl}) is calculated as follows,

$$E_{\text{cl,rel}} = E_{\text{slab}}(A) + E_{\text{slab}}(B) - nE_{\text{bulk}}, \quad (1)$$

where E_{slab} and E_{bulk} are the total energies of a relaxed slab and the bulk, respectively. A and B denote the complementary terminations. The cleavage energy is divided equally between each different two terminations. The results of calculated cleavage energies of the MnTiO₃-(104) (Mn/O2, TiO/Mn, O1/O1 and O2/TiO) and MnTiO₃-(110) (O2/MnTi and O1/O1) are illustrated in Figure S4. The results directly indicate that the MnTiO₃-(104) terminations (except Mn/O2 S4a) are energetically favourable cleavage planes compared to the MnTiO₃-(110) terminations. Based on these results, we can consider (104) to be more stable than the (110) surface. In the subsequent phase of our investigation into termination stability for the (104) surface plane, we propose employing the adsorption energy per layer as a indicator of surface stability. Specifically, we examine the adsorption energies for a sequential addition of O1, TiO, O2, and Mn layers starting from a Mn termination, which manifest adsorption energies of -10.65, -11.32, -4.29, and 3.62 eV per layer, respectively (as visually presented in Figure S5). The outcome from this assessment suggests that both TiO and O1 terminations exhibit a heightened potential to serve as the most stable selection.

^a Institute of Advanced Ceramics, Hamburg University of Technology, 21075 Hamburg, Germany. E-mail: doaa.ahmed@tuhh.de

^b Research, Development and Application Center (SARGEM), Sakarya University, Esentepe, Sakarya 54187, Turkey.

^c Department of Metallurgical and Materials Engineering, Engineering Faculty, Sakarya University, Esentepe, Sakarya 54187, Turkey.

^d Institute of Soft Matter Modeling, Hamburg University of Technology, 21075 Hamburg, Germany. E-mail: gregor.feldbauer@tuhh.de

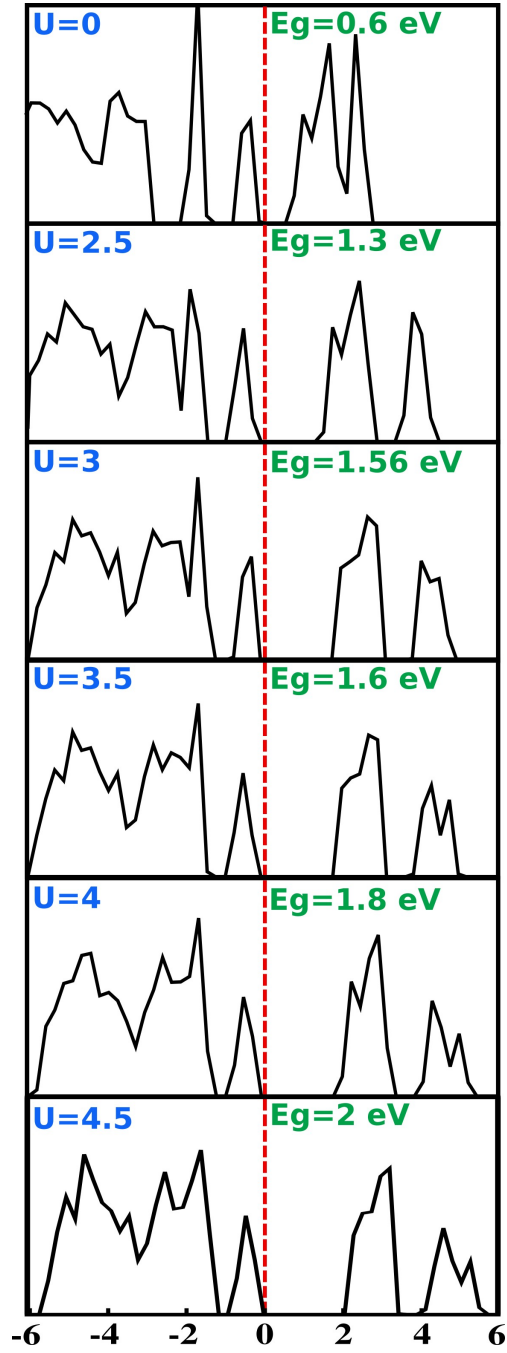


Fig. S1 Density of States (DOS) analysis and the band gap values of the MnTiO_3 using GGA+U functional with $U_{\text{H,eff}}$ values of 0, 2.5, 3, 3.5, 4, and 4.5.

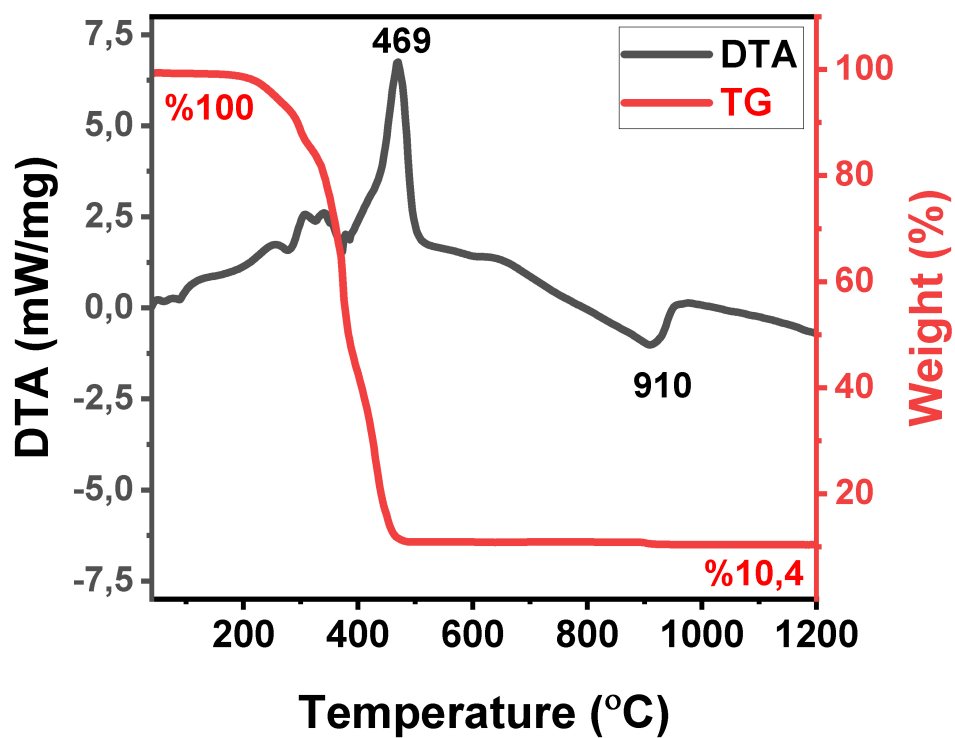


Fig. S2 DTA-TG curves of the precursor

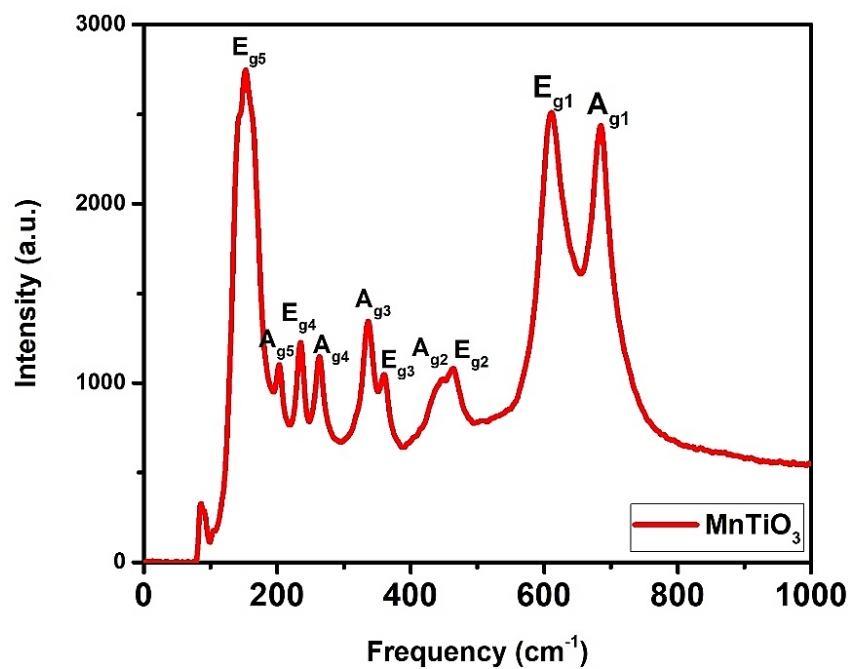


Fig. S3 Raman spectrum of the as-synthesized MnTiO₃ powders

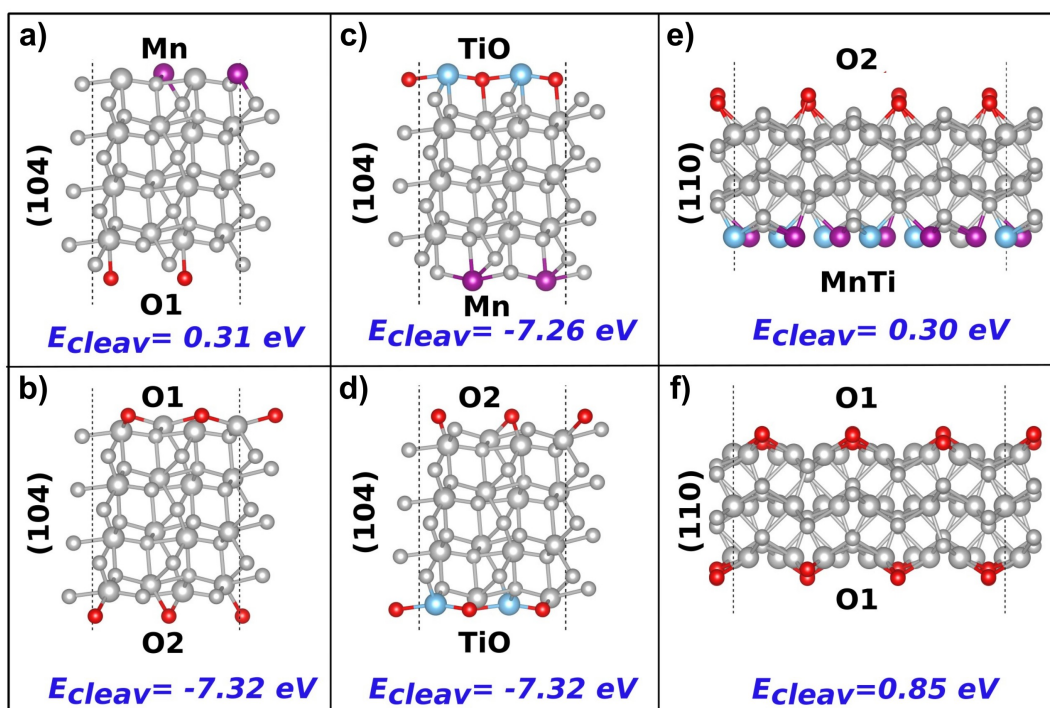


Fig. S4 The calculated cleavage energies (E_{cleav}) for MnTiO₃ slabs with (104) surface of a) Mn-O1 b) O1-O2, c) TiO-Mn, and d) O2-TiO terminations. And for (110) surface of e) O2-MnTi and f) O1-O1 terminations.

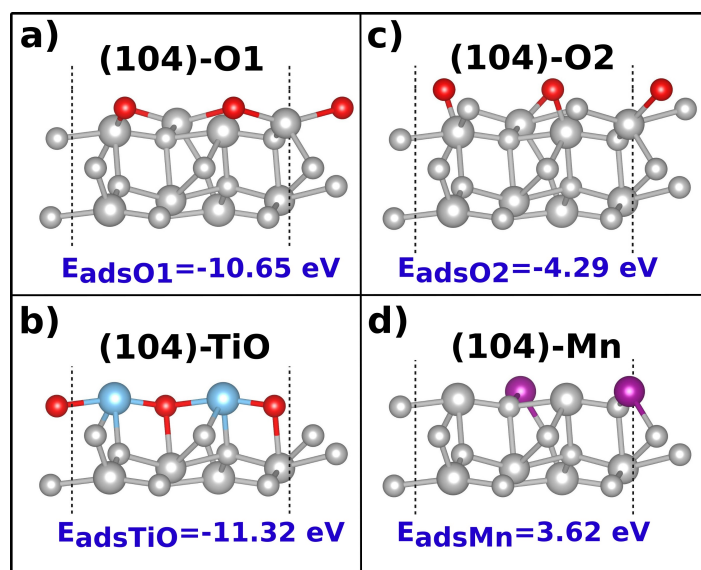


Fig. S5 The calculated adsorption energy per layer for MnTiO₃ with (104) surface of a) O1 b) TiO, c) O2, and d) Mn terminations.

Table S1 Adsorption energies for various reaction steps in the lithiation process. The calculated reaction energies are derived from the difference between the total energy of the surface with adsorbates and the sum of the isolated energies of the surface and adsorbates.

Adsorbate	Reaction Path	Calculated Adsorption Energy	Adsorption Energy (eV)
$E_{\text{ads}}(\text{Li})$	surface* + Li	$E_{\text{ads}} = E_{\text{surface}^*+\text{Li}} - (E_{\text{surface}^*} + E_{\text{Li}})$	-1.50
$E_{\text{ads}}(\text{O}_2)$	surface* + O₂	$E_{\text{ads}} = E_{\text{surface}^*+\text{O}_2} - (E_{\text{surface}^*} + E_{\text{O}_2})$	-2.88
$E_{\text{ads}}(\text{LiO}_2)$	surface_{O₂} + Li	$E_{\text{ads}} = E_{\text{surface}^*+\text{O}_2+\text{Li}} - (E_{\text{surface}^*+\text{O}_2} + E_{\text{Li}})$	-2.88
$E_{\text{ads}}(\text{Li}_2\text{O}_2)$	surface_{LiO₂} + Li	$E_{\text{ads}} = E_{\text{surface}^*+\text{LiO}_2+\text{Li}} - (E_{\text{surface}^*+\text{LiO}_2} + E_{\text{Li}})$	-1.89
$E_{\text{ads}}(\text{Li}_2\text{O}_4)$	surface_{Li₂O₄} + O₂	$E_{\text{ads}} = E_{\text{surface}^*+\text{Li}_2\text{O}_4+\text{O}_2} - (E_{\text{surface}^*+\text{Li}_2\text{O}_4} + E_{\text{O}_2})$	-2.83
$E_{\text{ads}}(\text{Li}_3\text{O}_2)$	surface_{Li₂O₂} + Li	$E_{\text{ads}} = E_{\text{surface}^*+\text{Li}_2\text{O}_2+\text{Li}} - (E_{\text{surface}^*+\text{Li}_2\text{O}_2} + E_{\text{Li}})$	-1.18
$E_{\text{ads}}(\text{Li}_3\text{O}_4)$	surface_{Li₂O₄} + Li	$E_{\text{ads}} = E_{\text{surface}^*+\text{Li}_3\text{O}_4} - (E_{\text{surface}^*+\text{Li}_3\text{O}_4} + E_{\text{Li}})$	-4.38
$E_{\text{ads}}(\text{Li}_4\text{O}_4)$	surface_{Li₃O₄} + Li	$E_{\text{ads}} = E_{\text{surface}^*+\text{Li}_4\text{O}_4} - (E_{\text{surface}^*+\text{Li}_4\text{O}_4} + E_{\text{Li}})$	-7.50

Reference

1. K. Kołodziejak, A. Niewiadomski, H. B. Surma, J. Sar, P. Piotrowski, E. Talik and D. A. Pawlak, J. Solid State Chem., 2024, 338, 124839.